Protein Science (1999), *8*:788–799. Cambridge University Press. Printed in the USA.

Helicity of α(404–451) and β(394–445) tubulin C-terminal recombinant peptides

M. ANGELES JIMENEZ,[1] JUAN A. EVANGELIO,[2] CARLOS ARANDA,[3] ADAMARI LOPEZ-BRAUET,[3] DAVID ANDREU,[4] MANUEL RICO,[1] ROSALBA LAGOS,[3] JOSE M. ANDREU,[2] AND OCTAVIO MONASTERIO[3]

[1]Instituto de Estructura de la Materia, CSIC, Serrano 119, 28006 Madrid, Spain
[2]Centro de Investigaciones Biológicas, CSIC, Velazquez 144, 28006 Madrid, Spain
[3]Departamento de Biología, Facultad de Ciencias, Universidad de Chile, Casilla 653, Santiago, Chile
[4]Departament de Química Orgánica, Universitat de Barcelona, Martí i Franqués 1-11, 08082 Barcelona, Spain

(RECEIVED October 26, 1998; ACCEPTED January 13, 1999)

Abstract

We have investigated the solution conformation of the functionally relevant C-terminal extremes of α- and β-tubulin, employing the model recombinant peptides RL52α3 and RL33β6, which correspond to the amino acid sequences 404–451(end) and 394–445(end) of the main vertebrate isotypes of α- and β-tubulin, respectively, and synthetic peptides with the α-tubulin(430–443) and β-tubulin(412–431) internal sequences. α(404–451) and β(394–445) are monomeric in neutral aqueous solution (as indicated by sedimentation equilibrium), and have circular dichroism (CD) spectra characteristic of nearly disordered conformation, consistent with low scores in peptide helicity prediction. Limited proteolysis of β(394–445) with subtilisin, instead of giving extensive degradation, resulted in main cleavages at positions Thr409–Glu410 and Tyr422–Gln423–Gln424, defining the proteolysis resistant segment 410–422, which corresponds to the central part of the predicted β-tubulin C-terminal helix. Both recombinant peptides inhibited microtubule assembly, probably due to sequestration of the microtubule stabilizing associated proteins. Trifluoroethanol (TFE)-induced markedly helical CD spectra in α(404–451) and β(394–445). A substantial part of the helicity of β(394–445) was found to be in the CD spectrum of the shorter peptide β(412–431) with TFE. Two-dimensional ^{1}H-NMR parameters (nonsequential nuclear Overhauser effects (NOE) and conformational CαH shifts) in 30% TFE permitted to conclude that about 25% of α(404–451) and 40% of β(394–451) form well-defined helices encompassing residues 418–432 and 408–431, respectively, flanked by disordered N- and C-segments. The side chains of β(394–451) residues Leu418, Val419, Ser420, Tyr422, Tyr425, and Gln426 are well defined in structure calculations from the NOE distance constraints. The apolar faces of the helix in both α and β chains share a characteristic sequence of conserved residues Ala,Met(+4),Leu(+7),Tyr(+11). The helical segment of α(404–451) is the same as that described in the electron crystallographic model structure of $\alpha\beta$-tubulin, while in β(394–451) it extends for nine residues more, supporting the possibility of a functional coil $\rightarrow$ helix transition at the C-terminus of β-tubulin. These peptides may be employed to construct model complexes with microtubule associated protein binding sites.

Keywords: CD and NMR; MAPs binding; recombinant peptides; tubulin C-termini

The $\alpha\beta$-tubulin dimers are the building blocks of microtubules, which are dynamic cytoskeletal fibers central to cytoplasmic organization, motility, and chromosome segregation in eukaryotic cells. The C-terminal domains of α- and β-tubulin contain both the longest regions of conserved sequence; these regions are predicted to be helical. Also present in the C-terminal domains are the hypervariable highly acidic zones comprising the 10–20 most C-terminal residues (discussed by de Pereda et al., 1996), which contain the tubulin isotype-defining sequences and most of the known post-translational modifications (reviewed by Ludueña, 1998). These characteristic C-terminal sequences (Ponstingl et al., 1979) are exclusively found in the tubulin family, and are functionally very important because they support the binding of proteins through which microtubules interact with other cell components, including microtubule associated proteins (MAPs) (Serrano et al., 1984; Littauer et al., 1986), which associate to microtubules by means of unprecisely defined multivalent interactions (Butner &

Reprint requests to: Jose M. Andreu, CIB, CSIC, Velazquez 144, 28006 Madrid, Spain; e-mail: j.m.andreu@fresno.csic.es.

Abbreviations: BSA, bovine serum albumin; CD, circular dichroism, COSY, correlation spectroscopy; EDTA, ethylenediaminetetraacetic acid; EGTA, ethyleneglycol-bis(β-aminoethyl ether)-*N,N,N′,N′*-tetraacetic acid; GTP, guanosine-5′-triphosphate; HPLC, high-performance liquid chromatography; IPTG, isopropyl-β-D-thiogalactophyranoside; MAP, microtubule associated protein; MTP, microtubule protein; NOE, nuclear Overhauser effect; NOESY, nuclear Overhauser effect spectroscopy; PDB, Protein Data Bank; PMSF, phenylmethylsulfonylfluoride; RMSD, root-mean-square deviation; RP-HPLC, reversed-phase HPLC; 2D, two-dimensional; TFE, trifluoroethanol; TOCSY, total correlation spectroscopy; TPPI, time proportional phase incrementation; UV, ultraviolet.

Kirschner, 1991; Novella et al., 1992; Gustke et al., 1994; Chau et al., 1998), and microtubule motor proteins (Paschal et al., 1989; Marya et al., 1994; Larcher et al., 1996), whose interactions and motion along microtubules are being very actively investigated (Mandelkow & Johnson, 1998).

Microtubule assembly is inhibited by Ca^{2+}, which acts indirectly via MAP-2 (Krueger et al., 1997) and tau phosphorylation (Fleming & Johnson, 1995), as well as by direct destabilization of growing microtubule ends (O'Brien et al., 1997). It has been hypothesized that Ca^{2+} may increase the rate of GTP hydrolysis within the stabilizing GTP-tubulin cap (O'Brien et al., 1997), and it has actually been shown that Ca^{2+} stimulates the GTPase activity of purified unassembled tubulin (Soto et al., 1996). The higher affinity Ca^{2+} binding sites (Solomon, 1977) of mammalian brain tubulin had been mapped to its acidic C-terminal zones by limited proteolysis with subtilisin (Serrano et al., 1986), as well as with chemical modification (Mejillano & Himes, 1991). Limited proteolysis with subtilisin predominantly cleaves the hypervariable 10 to 20 C-terminal residues of each tubulin chain, generating the C-terminally modified protein (S-tubulin) and releasing short peptides (S-peptides), which are largely heterogeneous (Sackett et al., 1985; de la Viña et al., 1988; Redecker et al., 1992; Lobert et al., 1993; Ortiz et al., 1993; de Pereda & Andreu, 1996; de Pereda et al., 1996).

We have designed, expressed, and chemically synthesized well-defined model fragments of the α- and β-tubulin C-terminal sequences, including the C-terminal helix and the acidic end of the chain, to make detailed studies of the structure–function of tubulin C-ends possible. Employing subtilisin proteolysis, CD, and NMR methods, we have characterized their helix forming ability in solution structure. During the preparation of this manuscript, the electron crystallographic unrefined model structure of αβ-tubulin dimers, missing the hypervariable C-terminal residues, has been presented (Nogales et al., 1998). The isolated, post-translationally unmodified, tubulin C-terminal model sequences are initially unordered, yet inhibit microtubule assembly, and form well-defined α-helices in TFE solution, mimicking the conformation within the protein.

Results and discussion

C-terminal constructs of α- and β-tubulin. Physico-chemical properties

Recombinant peptides containing the C-terminal sequences of the major vertebrate brain isotypes of α-tubulin (hkα1) and β-tubulin (cβ2) were produced in bacteria. Comparison of the results provided by N-terminal sequencing with the amino acid sequence encoded in their respective plasmids (Fig. 1) showed that the α-tubulin fragment RL52α3 actually starts at Phe404, and therefore consists of the 48 C-terminal residues of α-tubulin (404–451); this is possibly a result of bacterial proteolysis (C. Gómez, C. Aranda, R. Lagos, & O. Monasterio, unpubl. obs.). The β-tubulin construct RL33β6 misses the N-terminal Met and consists of the 52 C-terminal residues of β-tubulin (394–445), preceded by the sequence ARIRAP from the plasmid construction. Amino acid analyses and the number of Trp and Tyr residues confirmed their composition. The shorter peptide sequences α-tubulin (430–445) and β-tubulin (412–431) (underlined in Fig. 1) were chemically synthesized by solid-phase methods. Electrospray mass spectrometry gave molecular masses of 5,478.77 ± 0.27 Da for the α(404–451) recombinant fragment (theor. 5,478.8 Da) and 6,770.23 ± 0.55 Da for the β(394–445) recombinant fragment (theor. 6,770.7 Da). Both C-terminal fragments of α- and β-tubulin were monomeric in aqueous buffer solution, as indicated by sedimentation equilibrium measurements (not shown). Their apparent molecular masses were 4,400 and 6,600 Da respectively (10 mM Mes, 0.15 M NaCl, pH 6.5). The value for the α-tubulin fragment is an underestimation, possibly due to nonideality, supported by the fact that lower values were determined for both acidic fragments at low ionic strength (10 mM Mes pH 6.5).

Helical predictions

The predictions of helical population of the α- and β-tubulin recombinant and synthetic tubulin peptides made with the program Agadir (Muñoz & Serrano, 1994) are compared with the secondary structure prediction in the C-terminal zones of the α- and β-tubulin families of proteins made with the PHD method (Rost & Sander, 1993) in Figure 1A and 1B, respectively. Both methods, even designed for clearly different applications, detect marked helical propensities at similar positions in the α-tubulin (417/420–433/435) and β-tubulin (405–430/431) sequences (residues with Agadir helicity ≥1% or PHD helical prediction estimated accuracy >82%). The percent helix predicted by Agadir for each peptide in solution is: α(404–451) 1.8%, α(430–445) 0.0%, β(394–445) 1.2%, β(412–431) 1.1%. On the other hand, PHD predicts that these parts of the protein have 44, 37, 58, and 100% of their residues, respectively, in helical conformation. These conserved C-terminal helices are among the largest predicted secondary structure elements in tubulin (de Pereda et al., 1996). Note that each Agadir and PHD predictions make good sense in comparison with different experimental results, as will be shown later. Although coiled-coil predictions with the program COILS give high scores for these amphipatic helices (Lupas et al., 1991), particularly the sequences α-tubulin (414 to ~435) and β-tubulin (403 to ~430, extending toward the C-end), which parallels the PHD helical prediction, these sequences score poorly with the program PAIRCOIL (Berger et al., 1995). Interestingly, helical wheel projections of the sequences show that the apolar faces of these helices include four identical amino acid residues located in equivalent positions in both cases. These are α-tubulin Ala421, Met425, Leu428, and Tyr432, and β-tubulin Ala411, Met415, Leu418, and Tyr422 (Fig. 3C,D), which are, with the N-terminal amino acids, the only residues of this helix common to both tubulin sequences.

Limited proteolysis of the recombinant β-tubulin (394–445) fragment

To biochemically probe the solution structure of the C-terminal 52 residues of β-tubulin and to test the helical prediction, the β-tubulin (394–445) fragment was subjected to very mild proteolysis with subtilisin. We had expected that this relatively unspecific protease, which is frequently employed to cleave tubulin C-termini, would give extensive proteolysis of the peptide if it were fully disordered. However, proteolysis of the construct by 0.05% (w/w) subtilisin gave a limited series of well-defined fragments (Fig. 2A). The main eight HPLC peaks (more than 70% of the total peptide absorption at 215 nm in the chromatogram) were identified by near UV absorption (Tyr, Trp) and N-terminal microsequencing (Fig. 2B), and aligned onto the sequence of the β-tubulin C-terminal construct (see numbered horizontal lines in Fig. 2C). The prote-

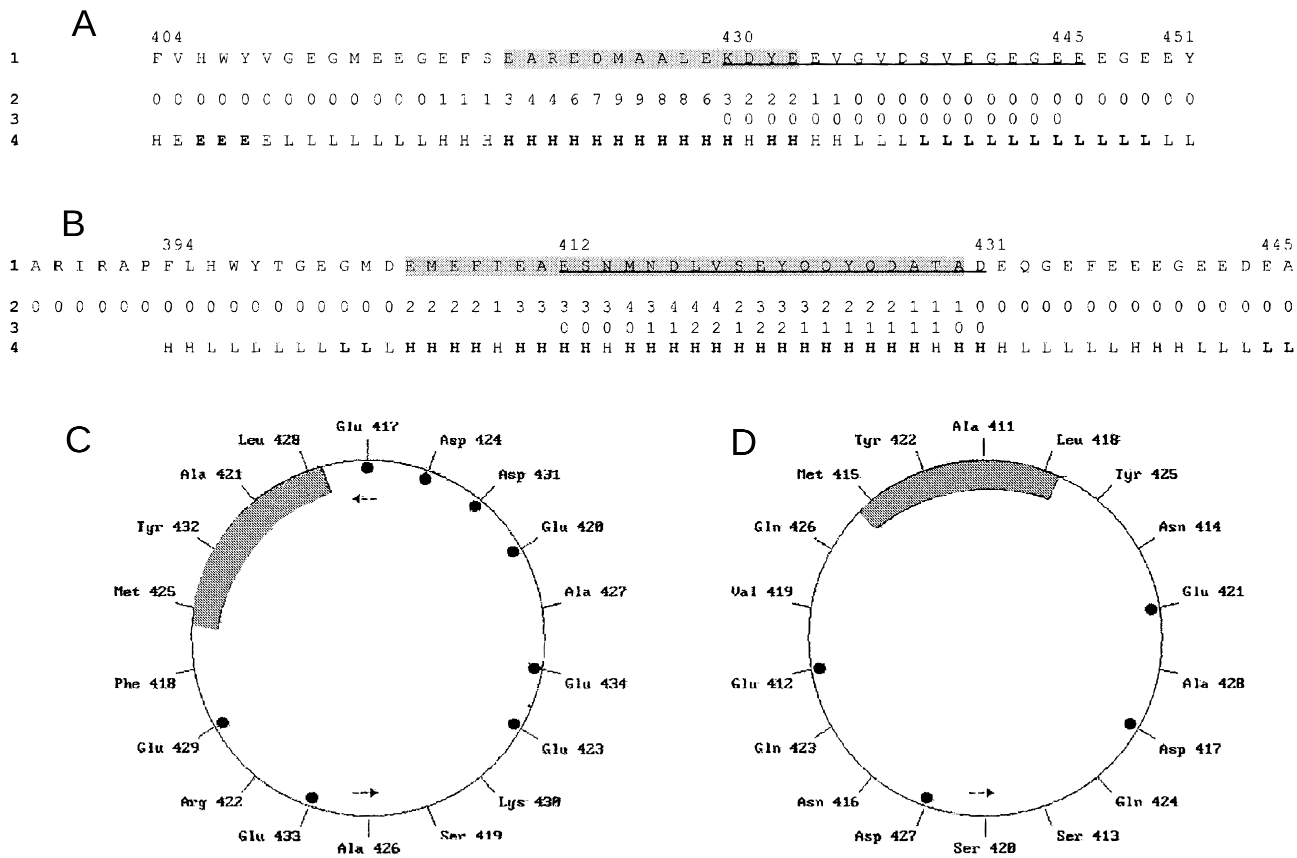

Fig. 1. Tubulin C-terminal constructs. The sequences of the RL52α3 and RL33β6 recombinant peptides are shown by (**A**) and (**B**), respectively (lines 1, one-letter code). The N-terminal amino acid sequence determined for the α-tubulin fragment was FVHWYVG EGMEEGEF(S)(E)ARE(D)MAALXXD(Y) . . . , lacking the plasmid encoded N-terminal sequence MARIRAPWARLDHKFDLMY AKRA. The result of sequencing the β-tubulin fragment was ARIRAPFLHWYTGEGMDEMEFTEEAESNMNDLVSEYQQYQXAT ADEQGEFEXXG . . . , missing N-terminal Met residue. The peptides α(430–445) and β(412–431) (underlined) were chemically synthesized. The secondary structure predictions of the sequences α(404–451) and β(394–445) are also shown by (**A**) and (**B**), respectively. Lines 2, helicity of each residue predicted by the program AGADIR (Muñoz & Serrano, 1994), expressed as percentage (%, rounded off by excess). Lines 3, helicity of each residue predicted for the shorter synthetic peptides. Lines 4, secondary structure predicted for the tubulin C-terminal zones by the program PHD (Rost & Sander 1993). H: α-helix, E: extended, L: loop. Bold symbols indicate residues with predictive accuracy over 82%. The sequences with strong helical predictions are shadowed gray. (**C,D**) Helical wheel schemes of the sequences α(417–434) and β(411–428), respectively, displayed with the PC-Gene computer program (release 6.0, IntelliGenetics Inc.). The incremental angle was 100°. The hydrophobicity values were -0.31 and -0.18, and the hydrophobic moment values were 0.26 and 0.28 for the α and β sequences, respectively. The filled circles indicate acidic residues. The residues indicated by the shaded arc are located in equivalent position in both sequences.

olysis data indicated that the main cleavages are at positions Tyr422–Gln423–Gln424 and Thr409–Glu410, defining a resistant segment 410–422, which is contained within fragments 3 and 6, and corresponds to the central part of the predicted helix 405–431 (see scheme in Fig. 2C), even under aqueous solution conditions where a significant helical population is not detected by CD (see below). These results suggest some transient helical structures in this region of the peptide when dissolved in water, which might correspond to the formation of nascent helices (Dyson et al., 1988). Cleavage at position Leu418–Val419 and possibly at Trp397–Tyr398 are minor or secondary processes. Note that further degradation of the sequence 424–445 (fragment 1) at the C-terminal end was unexpectedly not observed. The proteolysis data from the construct can be employed as a model of C-terminal modification of tubulin by subtilisin, which gives a complex fragment mixture. In fact, this and other information has permitted the localization of the main C-terminal cleavage points of β-tubulin by subtilisin at positions 409–410, 422–423, and 433–434, with a maximal uncertainty of +/− three residues (de Pereda & Andreu, 1996).

CD spectroscopy of the α- and β-tubulin C-terminal fragments

The average secondary structure of the C-terminal tubulin sequences in solution was examined by circular dichroism (CD). The tubulin C-terminal fragment α(404–451) had negligible helical structure in aqueous buffer (Fig. 3A, spectra a and d). Addition of the helix inducing cosolvent trifluoroethanol (TFE) (Nelson & Kallenbach, 1986; Luo & Baldwin, 1997) resulted in the appearance of a clear helical component (observe the minima at 208 and 220 nm and the increase of ellipticity at 195 nm in spectra b and c compared to spectrum a in Fig. 3A), mainly at the expense of the

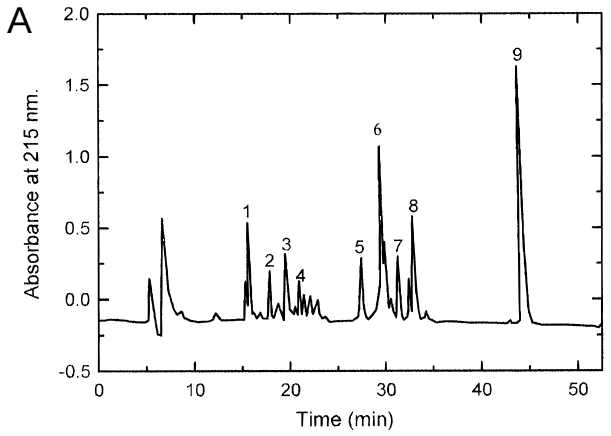

B

PEAK	TIME (min)	SEQUENCE
1	15.5	QQYQDATADEQGEFEE...+ QYQDATADEQGEFEE...
2	17.7	VSEYQQYQDAT...
3	19.5	EAESNMNDL
4	21.3	YTGEGEMDEMEFT
5	27.3	*(UNCLEAVED PEPTIDE)*
6	29.4	ARIRAPFLHWYFGEMDEMEFTEAES...
7	30.9	ARIRAPFLHWY...
8	32.5	ARIRAPFLHWYTGE...
9	43.6	*(PMSF)*

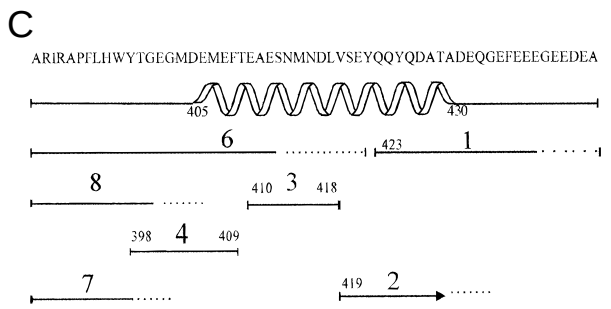

Fig. 2. A: HPLC separation of the products of limited proteolysis of the β-tubulin recombinant peptide 394–445 (0.5 mg mL^{-1}) with 0.05% (w/w) subtilisin in 50 mM Mes, 0.5 mM $MgCl_2$, 1 mM EGTA, pH 6.5 during 20 min at 25 °C. The reaction was stopped with 1 mM PMSF. **B**: N-terminal sequencing of each major fragment (peak 4 was determined from a different experiment). **C**: Alignment of the fragments (horizontal lines) onto the peptide sequence and scheme explaining the results of proteolysis. The segment predicted to form an α-helix (Fig. 1) is indicated. Proteolysis time course experiments (0.05 and 0.1% subtilisin, 5 to 40 min; not shown) indicated that fragment 6 and its complementary fragment 1 were present from the start of proteolysis. Decrease of fragment 6 coincided with an increase of fragment 3 and especially fragment 8 (becoming dominant at longer times); hence, they are probably complementary. Fragment 4 was transient (maximum 8% of total at 10 min with 0.05% subtilisin). The short N-terminal fragment complementary to fragment 4 has not been detected. Fragment 2 appeared last, and reached a maximum of 5%. Fragments 7 and 8 may be generated both from fragment 6 and directly from the complete sequence.

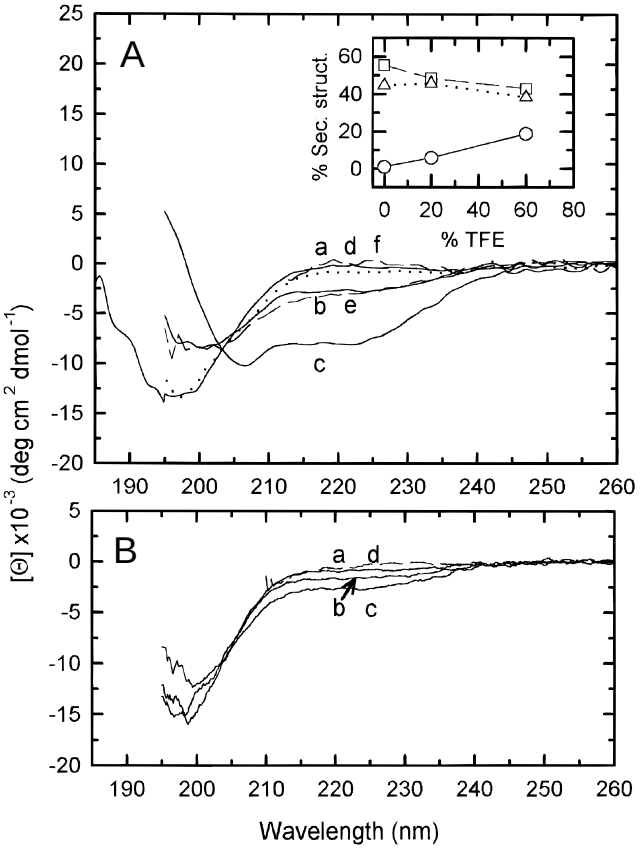

Fig. 3. CD spectra of (**A**) α(404–451) and (**B**) α(430–445) in 10 mM Mes pH 6.5, 25 °C. Line a, average of different spectra acquired with 1.0 and 0.1 mm cells; Line b, in the same buffer with a 20% TFE; Line c, 60% TFE; Line d (dashed line), in 6 M GuHCl; Line e (dashed line), in 10 mM Mes pH 2; Line f (dotted line), in 10 mM Mes pH 6.5, 1 mM Ca^{2+}. Analysis of CD spectrum (Line a) in **A** with the CCA (Perczel et al., 1992) or Yang et al. (1986) methods indicated negligible helix, 55 or 47% disordered structure, 39 or 24% beta sheet and 5% other or 30% turn components, respectively. Inset in **A:** percentage of secondary structure as estimated by the CCA method at increasing concentrations of TFE (0, 20, 60%). ○, α-helix; □, disordered; △, rest of structures.

disordered fraction. The estimated helical content was approximately 15 to 20% in 60% TFE. A weaker helix induction obtained by lowering the pH from 6.5 to 2, presumably results from a reduction of the electrostatic repulsion among ionized side chains of the very abundant acidic residues (line e, Fig. 3A). Addition of 1 mM $CaCl_2$ (line f) or lowering the temperature from 20 to 4 °C (not shown) did not modify the pH 6.5 spectrum. As a control, Figure 3B shows helical induction by TFE practically absent in the α-tubulin synthetic peptide 430–445, which marginally overlaps with the 417–435 helix predicted within the longer 404–451 sequence.

A small reproducible difference was observed between the CD spectrum of the tubulin C-terminal construct β(394–445) in buffer (Fig. 4A, line a) and in 6 M guanidinium chloride (GuHCl) (line d). The spectra in TFE (lines b and c in Fig. 4A) indicate a strong helical induction by this solvent. The estimated helical content in 30% TFE was 18 to 34%, and in 60% TFE it was 24 to 38%. A moderate helical induction was obtained by lowering the pH to 2 (line e). Lowering the temperature to 4 °C had a negligible effect (not shown), whereas addition of 1 mM $CaCl_2$ (line f) only modified the spectrum within experimental error.

Interestingly, the low helical peptide population predicted by the program Agadir (see above) is compatible with the CD analysis of the C-terminal zones of tubulin in aqueous buffer, whereas the helical prediction for the protein sequences by the PHD method

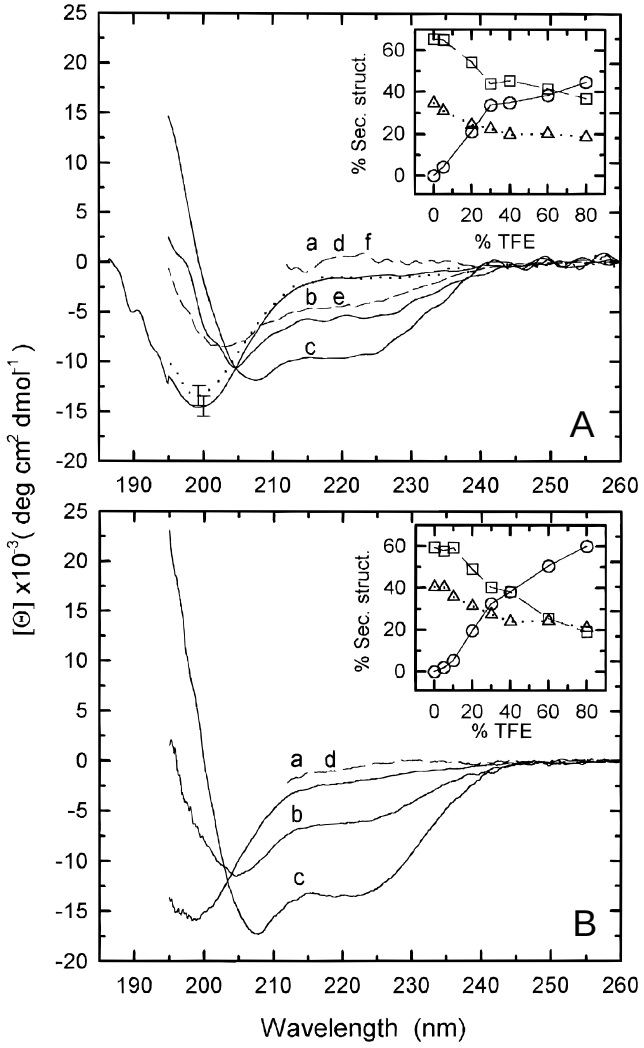

Fig. 4. CD spectra of (**A**) β(394–445) and (**B**) β(412–431) in 10 mM Mes pH 6.5, 25 °C. Line a, average of different spectra acquired with 1.0 and 0.1 mm cells; Line b, in the same buffer with a 20% TFE; Line c, 60% TFE; Line d (dashed line), in 6 M GuHCI; Line e (dashed line), in MES 10 mM pH 2; Line f (dotted line), in MES 10 mM pH 6.5 Ca^{2+} 1 mM. Analysis of spectrum a in **A** indicated negligible helical content, 35 or 48% disordered, 32 or 51% beta sheet, 33% other or 0% beta-turn components. Analysis of spectrum a in **B** indicated negligible helical content, 40 or 55% disordered, 28 or 26% beta sheet, and 31% other or 19% beta turn. Insets: percentage of secondary structure estimated with the CCA method at increasing concentrations of TFE (0, 5, 10, 20, 30, 40, 60, and 80%); ○, α-helix; □, disordered; △, rest of structures.

(see above) is qualitatively consistent with the CD in TFE. We reasoned that the isolated tubulin C-terminal zones in aqueous solution are incapable of adopting the significant helical conformation that they probably had in the protein micro-environment, which is mimicked by TFE. A qualitatively similar helix induction by TFE had been observed in a β-tubulin (400–445) peptide by Reed et al. (1992). However, the helical part of this zone of β-tubulin is predicted only to span approximately residues 405–431 (see above). To further test the prediction, the CD of synthetic peptide 412–431 was examined (Fig. 4B). The results are qualitatively similar to the longer β-tubulin (394–445) construct, the important difference being that the TFE-induced helical bands have nearly double ellipticity. The estimated helical content in 30% TFE was 22 to 32%, and in 60% TFE it was 35 to 51%. It can be concluded that the β-tubulin sequence 412–431 contributes substantially to the helicity of the larger 394–445 C-terminal zone. This is fully consistent with the prediction that the helicity of the β-tubulin C-terminal sequence 394–445 is localized in its central part in residues 405–431. However, the helix content estimated for the peptide 412–431 in TFE is roughly 60% that expected if all the helicity of the 52-residue sequence were concentrated in the 27 residues 405–431. This suggests that the isolated shorter peptide 412–431 may be less helical than the same sequence included within the longer peptide.

NMR conformational analysis of α- and β-tubulin fragments in 30% TFE solution

The conformational properties of the tubulin C-terminal peptides in 30% TFE solution were further analyzed by 2D ^{1}H-NMR methods. Several NMR parameters permit the identification of a preferred structure in a peptide, the strongest evidence coming from the NOE connectivities. Because a NOE connectivity between two protons is observed if they are spatially close together independently of their sequence proximity, the nonsequential NOE cross-correlations are indicative of some preferred, sufficiently populated conformation in which the corresponding protons are close together. The deviations of the δ-values measured for the peptide CαH protons with respect to those expected for nonstructured peptides (conformational CαH shift, $\Delta\delta = \delta_{\text{observed}} - \delta_{RC}$, ppm) provide additional information about the presence and nature of the preferred conformation adopted by a peptide. These deviations are negative in helices and positive in extended or β-sheet conformations (Case et al., 1994; Wishart & Sykes, 1994).

In addition to the sequential NOE connectivities used for assignment, a number of nonsequential NOE cross-peaks are observed in the NOESY spectra of the short peptide β(412–431) and of recombinant peptide β(394–445), in 30% TFE solution at pH 7.0, 25 °C (Figs. 5–7). In particular, the stretch of $\alpha Ni,i+2$, $\alpha Ni,i+3$, $\alpha Ni,i+4$, and $\alpha\beta i,i+3$ NOE connectivities, all of which are characteristic of helices, and the observed nonsequential $i,i+3$ and $i,i+4$ NOE connectivities involving side-chain protons indicate that these peptides adopt a significant population of a helical conformation in 30% TFE solution. Such helical conformation spans residues 415–430 in the short peptide β(412–431) and 408–431 in peptide β(394–445). The conformational CαH shifts obtained for segment 415–427 of peptide β(412–431) and for segment 410–427 of peptide β(394–445) are negative and large in absolute value ($|\Delta\delta| > 0.1$ ppm), which confirms the helix formation in the same regions where the NOEs characteristic of helix were identified (Figs. 6, 7). Helix populations were estimated from the average of the CαH shifts within the helical regions (Jiménez et al., 1993, 1994). The helix population adopted by the short peptide β(412–431) within region 415–430 was about a 38%, a value compatible with the CD estimation (35–51%, see above). Peptide β(394–445) adopts about 40% of helix within region 408–431 and 45% within region 415–430. Thus, the helix adopted by the longer peptide β(394–445) comprises the one formed by the short peptide (412–431), but with a slightly higher population, and is elongated at its amino-terminus. Most of the nonsequential NOEs involving side-chain protons observed in both peptides within their helical regions were identical (not shown).

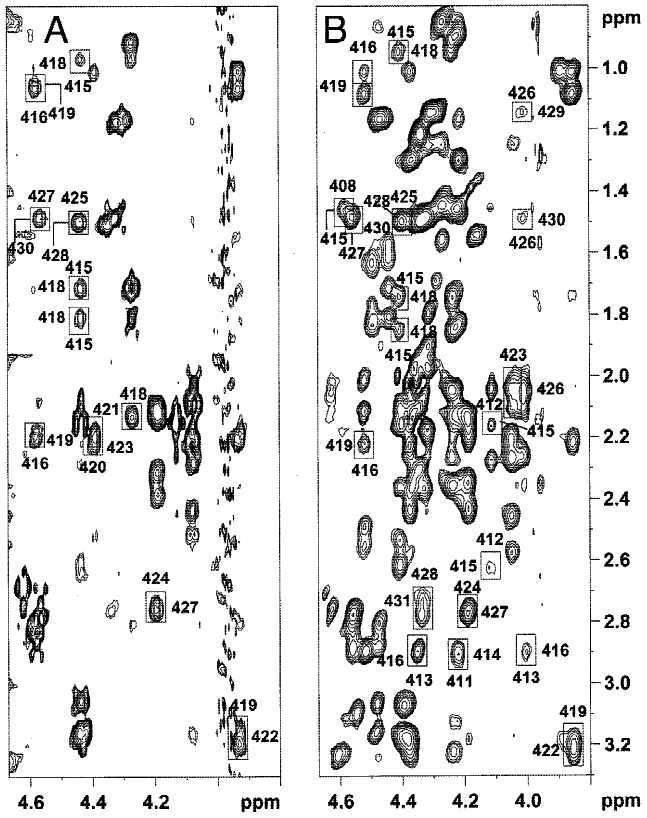

Fig. 5. Selected region of the 2D NOE spectrum of the peptides (**A**) β(412–441) and (**B**) β(394–445) in 30% TFE solution at pH 7.0 and 25 °C, with a 150 ms mixing time. Nonsequential $d_{\alpha N(i,i+2)}$ and $d_{\alpha N(i,i+3)}$ NOEs are boxed.

In peptide β(394–445), some nonsequential NOEs are also found in region 390/392–400, which indicates the existence of nonrandom conformation(s) within this region. Considering the amount of aromatic and hydrophobic residues in segment 390/392–400 (Fig. 7) and that many of the nonsequential NOEs in this segment involve side chains of this type of residues, such nonrandom conformation could be a hydrophobic cluster. However, the precise nature of the conformation or details about the arrangement of the side chains could not be determined because of the small number of nonsequential NOEs and the ambiguity of some of them. NOEs were observed between the aromatic protons of Phe394 and either the methyl group of Ala392 or one of the CδH protons of Ile390 (the later two show the same δ-value). The conformational CαH $\Delta\delta$ shifts of region 393–398, which are negative and relatively large in absolute value (Fig. 7), cannot be interpreted in terms of helix formation, due to the presence of four aromatic residues, three of them consecutive, within such a short segment. It is well known that the aromatic rings can significantly affect the δ-values of the nearby protons. The effect of the CαH protons of a residue preceding or following to an aromatic residue (Phe, Tyr, His, Trp) in a random coil peptide is upfield and varies from −0.03 to −0.13 ppm (Merutka et al., 1995).

Two stretches of nonsequential connectivities are apparent in the NOE summary of peptide α(404–451) in 30% TFE solution at pH 7.0 and 25 °C (Fig. 8). The stretch of $\alpha\beta(i,i+3)$ NOEs, together with the αN(425,428) NOE and the NOEs involving the side-chain protons of residues Met425 and Leu428 indicate the formation of a helix structure within region 418–431. The negative conformational $\Delta\delta$ CαH shifts found within segment 419–433 (Fig. 8) confirm the presence of a helix. Considering both the NOEs and the conformational shifts, we can conclude that the peptide α(404–451) forms a helix encompassing residues 418–432. The population of this helix is about 25%, estimated from the averaged CαH conformational shifts within zone 418–432 (Jiménez et al., 1993, 1994). As in region 390/392–400 of peptide β(394–445), the formation of a hydrophobic cluster can account for the nonsequential NOE connectivities involving the side-chain protons of the six N-terminal residues (four aromatic, two hydrophobic) of peptide α(404–451). The side-chain geometry within the cluster cannot be determined due to the small number of NOEs involving these residues, and the negative conformational CαH shifts (Fig. 8) in this zone cannot be interpreted in terms of any secondary structure because of the effect of the aromatic residues (Merutka et al., 1995, and above).

Because the ordered conformations identified above for the three peptide coexist in equilibrium with random-coil conformations, the NOE data cannot be interpreted in terms of a unique structure. Nevertheless, it is useful to perform the calculation of a limited number of structures compatible with the distance constraints derived from the NOEs as a way to visualize the conformational properties of the favored family of structures within the confor-

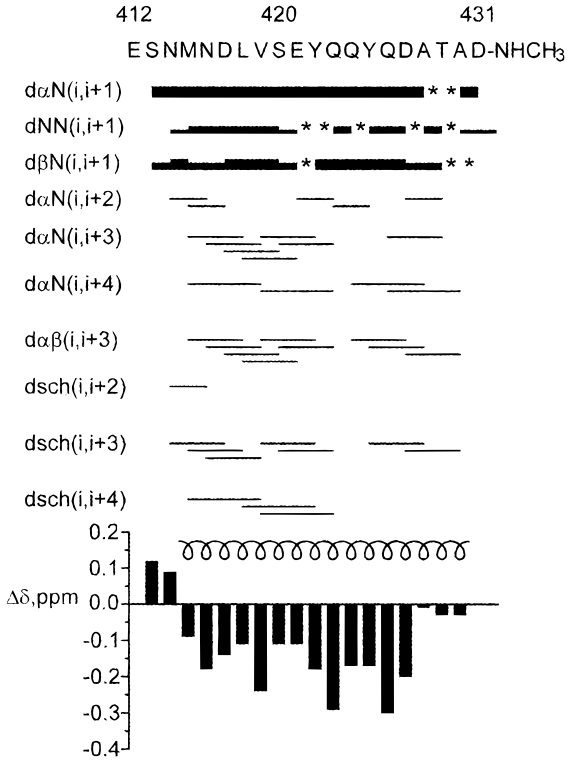

Fig. 6. Summary of NOE connectivities and conformational CαH $\Delta\delta$ shifts ($\delta_{\text{observed}} - \delta_{RC}$, ppm, where δ_{RC} are the δ corresponding to random coil peptides; Wüthrich, 1986), observed for the β-tubulin synthetic peptide β(412–441) in 30% TFE solution at pH 7.0 and 25 °C. The thickness of the lines reflects the intensity of the sequential NOE connectivities, i.e., weak, medium, and strong. An * indicates unobserved NOE connectivity due to signal overlapping, closeness to diagonal, or overlapping with solvent signal; dsch indicates NOE connectivities involving side chains.

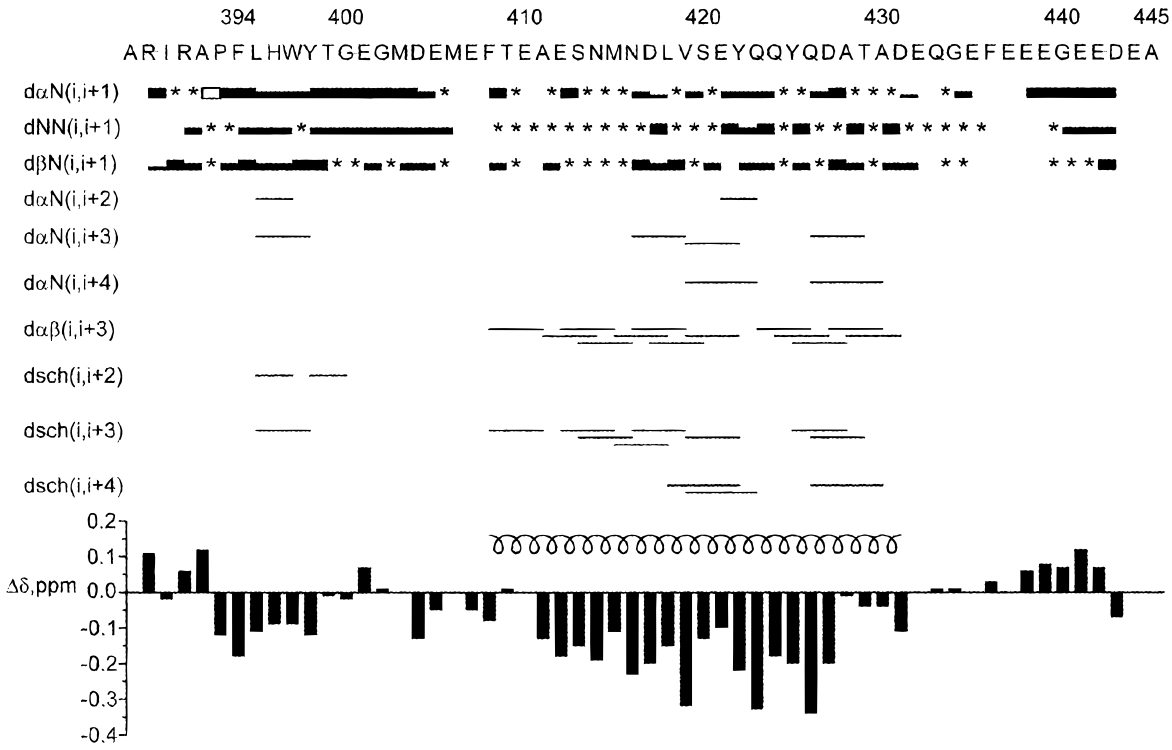

Fig. 7. Summary of NOE connectivities and conformational shifts observed for the β-tubulin construct β (394–445) in 30% TFE solution at pH 7.0 and 25 °C (see Fig. 6).

Fig. 8. Summary of NOE connectivities and conformational shifts observed for the α-tubulin construct α(405–451) in 30% TFE solution at pH 7.0 and 25 °C (see Fig. 6).

mational ensemble of a peptide. With this aim, structure calculations were performed on the basis of the nonsequential NOE connectivities observed. Sequential NOE connectivities were not included because the random conformations contribute to their intensity. The resulting structures of β(394–445) and α(404–451) contain a well-defined central helix region surrounded by disordered N- and C-segments. The RMSDs obtained for the 14 best calculated structures of β(394–445) (Fig. 9A) are 12.3 ± 3.2 Å for the backbone and 13.2 ± 3.0 Å including the side chains, and reduce to 2.8 ± 0.8 Å and 3.8 ± 0.8 Å, respectively, when only the residues belonging to the helix region (408–431) are considered. Side chains of some residues within the helix region (Leu418, Val419, Ser420, Tyr422, Tyr425, and Gln426) are relatively well defined, as indicated by a range of X_1 angle lower than 30°. The Ala411, Met415, Leu418, Tyr422, and Tyr 425 residues in the hydrophobic face of the helix are shown in Figure 9B. Structure calculation for the shorter β-tubulin peptide (412–431) gave a similar result with a shorter helical extension (not shown). In the case of α(404–451) (Fig. 9C), the RMSDs obtained for the best 14 calculated structures are 11.7 ± 2.6 Å for the backbone and 12.9 ± 2.5 Å including the side chains, and decrease to 2.4 ± 0.7 Å and 4.3 ± 0.8 Å, respectively, when only helical residues (418–432) are taken into account. Side chains are not well defined in this case.

Inhibition of microtubule assembly and Ca^{2+} binding by tubulin C-terminal fragments

The tubulin fragments characterized in this work include the conserved C-terminal helix followed by the hypervariable C-terminal end. The later can be cleaved from native tubulin with subtilisin, giving the heterogeneous shorter S-peptides (see the introduction). Both recombinant peptides α(404–451) and β(394–445) (62 μM) inhibited the assembly of microtubules from microtubule protein (2 mg/mL) to a similar extent (69 and 64%, respectively), as indicated by the plateau of turbidity time courses (see Supplementary material in Electronic Appendix Fig. SF2). The inhibition was larger in a second cycle of polymerization (81 and 77% inhibition, respectively, confirmed by measuring the nonpolymerized protein after pelleting the microtubules, which gave 83 and 82% inhibition, respectively). These results are more simply interpreted as due to interaction of both recombinant fragments with MAPs, reducing the binding of MAPs to microtubules and microtubule stabilization. The presence of secondary structure probably plays a role in the binding of these peptides to MAPs (Reed et al., 1992), even though initially the peptides are mostly disordered.

The recombinant peptides α(404–451) and β(394–445) were found to weakly bind Ca^{2+} (about 0.02 Ca^{2+} ion in columns equilibrated with 10 μM free $^{45}Ca^{2+}$; not shown), similarly to the low-affinity Ca^{2+} binding sites of tubulin (Solomon, 1977; Serrano et al., 1986).

Comparison of the conformation of the C-terminal zones in TFE solution and in zinc-induced tubulin crystals. Potential functional implications

After our CD and NMR structural analysis had been completed, a high-resolution electron crystallographic model structure of the $\alpha\beta$-tubulin dimer in zinc-induced sheets has been presented (Nogales et al., 1998). These 2D crystals correspond to an alternative way of tubulin polymerization, in which protofilaments have an antiparallel orientation, opposite to that in magnesium-induced microtubules. It is interesting to compare the two independently determined conformations of tubulin C-termini, in the isolated model peptide in TFE solution and in the protein polymer crystal structure. The extension of the C-terminal helix is identical in the case of α-tubulin, comprising in both cases residues 418–432. In the β-tubulin model peptide, this helix comprises positions 408–431 (essentially confirming prediction), extending at its C-terminus nine residues longer than in α-tubulin model peptide. This is also nine residues longer than in the unrefined crystal structure, where secondary structure has been identically assigned in both subunits (Fig. 3 in Nogales et al., 1998; see PBD file 1tub). The comparison is fully compatible with the notion that the helical potential of these tubulin sequences, which is marginally detected in aqueous solution, is expressed similarly with the TFE cosolvent and in the complete protein. The longer helix of the β-tubulin model peptide suggests an extension in the protein, supporting the possibility of a functional coil → helix transition at the C-terminal zone. This is consistent with an earlier proposal based on the mixed helix–coil prediction (Ponstingl et al., 1979; de Pereda et al., 1996; Fig. 1). Following this helix, the 19 and 14 C-terminal residues of the respective α- and β-tubulin model peptide are observed to be disordered by NMR. In the crystal structure (Nogales et al., 1998), the respective 10 and 18 C-terminal residues, together with the bulky post-translationally added polyglutamic acid chains (Eddé et al., 1990; Redecker et al., 1992), were simpy lost from the electron density map, possibly due to their disorder.

Despite the amphipatic character of this helix, no evidence of helix–helix pairing is found in the TFE solution or in the crystal structures. In the latter, this helix (H12) hydrophobically associates to the outer face of the tubulin monomer. The apolar side of this C-terminal α-helix (see Figs. 1C,D, 9B) is apparently satisfied by contacts with the N-terminal domain underneath (Nogales et al., 1998). A proton NMR study of the interaction of a MAP synthetic peptide with tubulin indicated that, in addition to the electrostatic interactions between basic and acid residues, there are interactions of MAP hydrophobic residues with aromatic residues at the tubulin C-terminal end, possibly Tyr422 and/or Tyr425 of β-tubulin (Kotani et al., 1990). These residues belong to the hydrophobic face of the C-terminal α-helix (Fig. 9B). It may be speculated that H12 and part of the C-terminal end, besides undergoing coil to helix transitions as exemplified by the model peptides in this study, might functionally switch from interacting with the underlying tubulin monomer to binding MAPs and motor proteins. Recombinant polypeptides of microtubule associated protein tau have been very recently shown to cross-link both with the extreme C-terminal 12 amino acids of tubulin and with a second site upstream, that is suggested to involve the C-terminal helix H12 (Chau et al., 1998). Studies combining recombinant soluble tubulin fragments (characterized for the first time in this study, to our knowledge) with constructs of the microtubule binding sites of tau (Chau et al., 1998; Novella et al., 1992) should enable the construction of representative model complexes leading to a high-resolution structural description of the key interactions of tubulin with microtubule-associated proteins.

Conclusions

Well-defined helix-forming zones in peptide models of the α- and β-tubulin C-termini extend from Phe418 to Tyr432 and Phe408 to Asp431, respectively, whereas the respective 19 and 14 C-terminal residues are disordered. The apolar side of the amphipatic helix

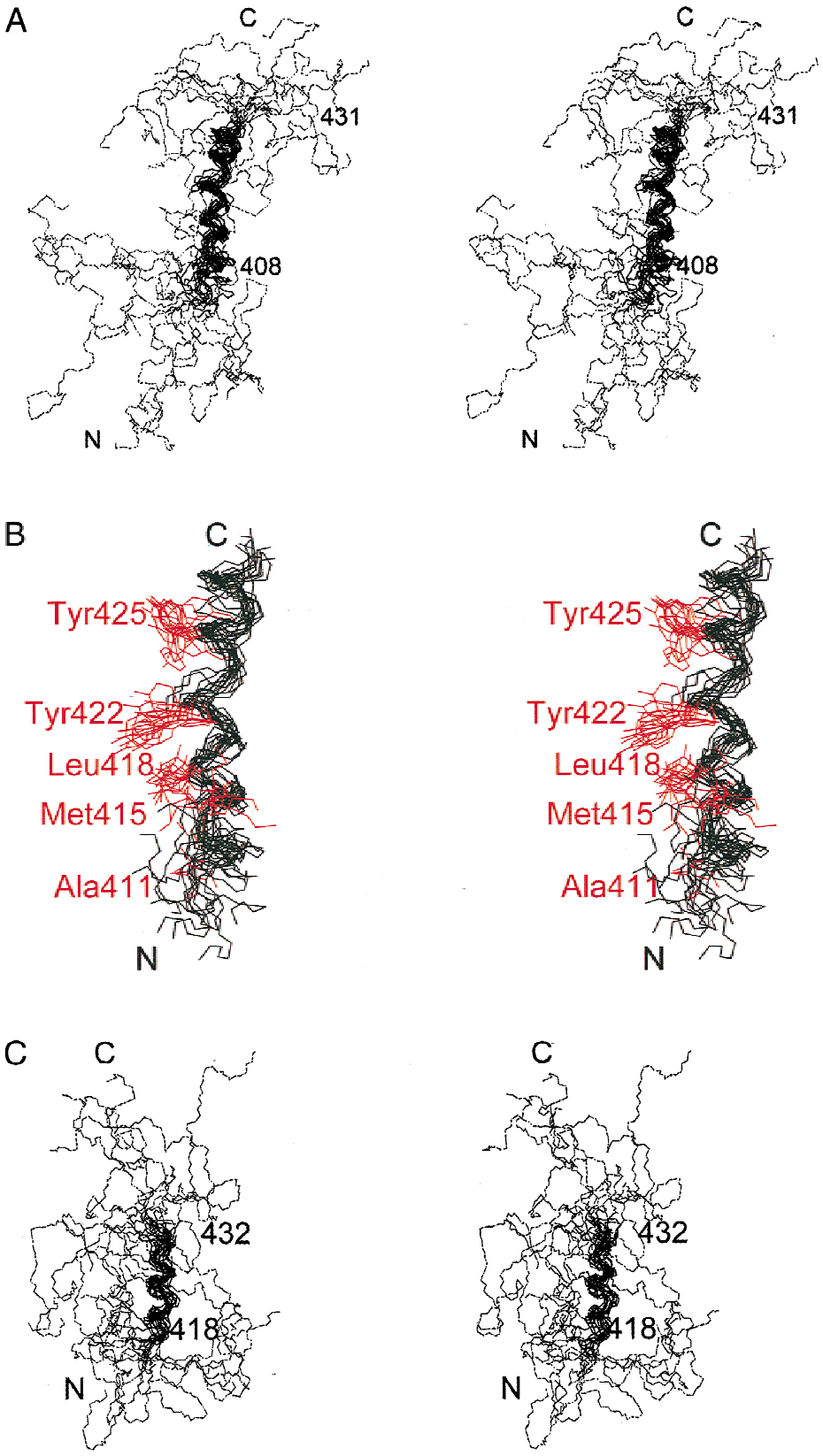

Fig. 9. **A**: Stereoview of the 14 best calculated structures for the tubulin construct β(394−445) superimposed over residues 410−432, showing the backbone nonhydrogen atoms of the entire polypeptide chain. Helix limits are indicated. **B**: Backbone nonhydrogen atoms of the helical region of this construct (residues 408−431, black lines) and side-chain atoms of residues Ala411, Met415, Leu418, Tyr422, and Tyr425 that belong to the hydrophobic face, shown in colored lines. The N- and C-termini are labeled. **C**: Stereoview of the 14 best calculated structures for the construct (404−451), showed similarly to **A**. The shorter helix limits are indicated.

includes characteristic Ala-Met(+4)–Leu(+7)–Tyr(+11) residues in both tubulin chains. The helical conformation depends on the environment: the isolated peptide sequences are predominantly disordered in neutral aqueous solution, but they are strongly helical in TFE solution or in the context of tubulin dimer crystals. Investigating the stability and structure of specific complexes of these tubulin fragments with relevant MAPs constructs offers an attractive possibility to better define the microtubule–MAPs interactions.

Materials and methods

Chemicals

GTP (type III), Mes, Pipes, EDTA, EGTA, IPTG (isopropyl-β-D-thiogalactopyranoside), rifampicin, subtilisin Carlsberg, and BSA (bovine serum albumin), were from Sigma (St. Louis, Missouri). D_2O and DCl were from M&G Chemicals (Stockport, United Kingdom). NaOD and 2,2,2-trifluoroethanol-d3 were from Cambridge Isotope Laboratories (Andover, Massachusetts). Ultrapure GuHCl was from Sigma and U.S.B. PMSF (phenylmethylsulfonylfluoride) was from Calbiochem (La Jolla, California). All other reagents were from Merck (Darmstadt, Germany), analytical or HPLC grade, except otherwise indicated.

Plasmids, bacterial expression and labeling, and chemical synthesis of C-terminal fragments of α- and β-tubulin

The hybrid plasmid pRL52α3 was constructed in two steps. The *Sma*I/*Pst*I cDNA fragment of the human α-tubulin gene α1 (Cowan et al., 1983) in a recombinant pPR322 derivative from cultured human keratinocytes (a gift from Dr. D.W. Cleveland, Johns Hopkins University) was ligated to the expression vector pT7-7 (generously provided by Dr. S. Tabor, Harvard Medical School) digested with the same enzymes. The resulting plasmid was digested with *Sma*I and *Stu*I, the 969 bp DNA fragment codifying between amino acids 64–387 was discarded, and the remaining fragment was circularized by intramolecular ligation, originating pRL52α3. This plasmid codifies for the 64 C-terminal amino acids of α-tubulin (388–451) preceded by the sequence MARIRAP (six residues from the vector and a proline generated by the construction). Plasmid pRL33β6 was constructed as described by González et al. (1996), starting from cDNA of the chicken β-tubulin cβ2 gene (Valenzuela et al., 1981), and codes for the 52 C-terminal residues of β-tubulin (394–445) preceded by the sequence MARIRAP. *Escherichia coli* BL21(DE3), a λ lysogen (Studier & Moffatt, 1986), was used as a host strain, and the induction was performed by the addition of 0.5 mM IPTG. Peptides were prepared starting from 12 L of cells essentially as described by Aranda (1994) and González et al. (1996). The specific labeling of each peptide was achieved using rifampicin (200 μg/mL) before adding ^{35}S-methionine (Tabor & Richardson, 1985).

The soluble fractions of the bacterially expressed peptides RL52α3 (30–40%) (C. González, R. Sánchez, R. Lagos, & O. Monasterio, unpubl. obs.) and RL33β6 (>95%) (González et al., 1996) were purified by ion exchange in DEAE-cellulose (chromatographed twice though DE-52, Whatmann, Maidstone, Kent, United Kingdom) followed by reverse-phase chromatography (in a Waters, Franklin, Massachusetts, Sep-Pak C-18 cartridge, eluted with a 10–50% acetonitrile gradient). The procedure gave a 53% yield of purified peptide (Aranda, 1994). These C-terminal fragments of α- and β-tubulin were 90% homogeneous in analytical HPLC (see Supplementary material in Electronic Appendix Fig. SF1). Fragment RL33β6 reacted with two different site-directed antibodies to the sequence (412–431) in a competition ELISA (not shown, see de la Viña et al., 1988) confirming that the expressed construction includes this sequence. The concentration of peptides RL33β6 and RL52α3 was determined spectrophotometrically, using an absorption coefficient of 9,530 M^{-1} cm^{-1} (280 nm, 6 M GuHCl) calculated (Edelhoch, 1967) for one Trp and three Tyr residues in the α(404–451) and β(404–451) sequences (see Fig. 1). The peptides with the pig brain α-tubulin(430–443) and β-tubulin(412–431) sequences were chemically synthesized as C-terminal amides employing solid-phase Merriefield procedures and were purified to HPLC homogeneity as described (Andreu et al., 1988; de la Viña et al., 1988). Their concentrations were measured spectrophotometrically with an extinction coefficient of 1,280 M^{-1} cm^{-1} (280 nm).

Analytical procedures

Peptides were analyzed by RP-HPLC with a 250 × 4.5 mm C18 column (Supelco, Bellefonte, Pennsylvania) in a Shimadzu LC-10AD system, eluted with gradients of acetonitrile in 50 mM ammonium acetate, pH 6.5. Electrospray mass spectra were obtained with a Fisons (Manchester, United Kingdom) VG Quattro spectrometer at the mass spectrometry service, University of Barcelona. N-terminal Edman microsequencing was made with an Applied Biosystems (Foster City, California) 477A sequencer equipped with on-line HPLC analysis of the phenylthiohydantoin derivatives, at the protein chemistry service, Centro de Investigaciones Biologicas (Madrid, Spain).

Analytical ultracentrifugation

Sedimentation equilibrium measurements were made with a Beckman Optima XL-A instrument equipped with absorbance optics, employing 12-mm double sector cells in an An60Ti rotor at 35,000 rpm, 20 °C. Attainment of equilibrium was verified by identical successive scans (280 and 230 nm) after 4 h of centrifugation of peptides. The concentration gradients were analyzed and whole-cell weight-average molecular masses obtained employing the programs EQASSOC (Minton, 1994) and Origin SINGLE (NONLIN; Johnson et al., 1981) supplied by Beckman, employing partial specific volume values (Laue et al., 1992) of α(404–451) and β(394–445) were 0.704 and 0.696 g mL^{-1}, respectively.

Circular dichroism spectroscopy

The far UV peptide CD spectra were acquired in a Jasco J720 dichrograph, employing 0.1 and 1 mm cells at 25 °C. Each spectrum is the accumulation of five scans (bandwidth 1 nm, scan rate 20 nm min^{-1}). The concentrations of the different tubulin peptide employed were comprised between 10 and 200 μM. The CD spectra were analyzed employing the Yang (Yang et al., 1986), CCA, and LINCOMB (Perczel et al., 1992) methods as described (de Pereda et al., 1996).

Nuclear magnetic resonance spectroscopy

NMR samples were prepared by solving the peptide in H_2O/D_2O 9:1 and adding the amount of 2,2,2-trifluoroethanol-d3 (Cam-

bridge Isotope Laboratories, Andover, Massachusetts) required to give 30% by volume. Peptide concentrations were about 2 mM. pH was adjusted to 7.0 by addition of minute amounts of DCl or NaOD. pH measurements were not corrected for isotope effects. Sodium 3-trimethylsilyl (2,2,3,3-$^2H_4$) propionate (TSP) was used as an internal reference. NMR experiments were performed on a Bruker (Karlsruhe, Germany) AMX-600 spectrometer. All the two-dimensional spectra were acquired in the phase-sensitive mode using the time proportional phase incrementation (TPPI) technique (Marion & Wüthrich, 1983) with presaturation of the water signal. COSY (Aue et al., 1976) and NOESY (Kumar et al., 1980) spectra were recorded using standard phase-cycling sequences. Short mixing times (150 ms) were used in the NOESY experiments to avoid spin-diffusion effects. TOCSY (Bax & Davis, 1985) spectra were acquired using the standard MLEV17 spin-lock sequence and a 80 ms mixing time. Size of the acquisition data matrix was 2,048 × 512 words in f_2 and f_1, respectively, and prior to Fourier transformation the 2D data matrix was multiplied by a phase-shifted square-sine bell-window function in both dimensions and zero-filled to 4,096 × 1,024 words. The phase shift was optimized for every spectrum.

^{1}H-NMR assignment

The assignment of the ^{1}H-NMR spectra of the peptides in 30% TFE solution at pH 7 and 25 °C was performed by using standard 2D sequence-specific methods (Wüthrich et al., 1984; Wüthrich, 1986). In the case of β(394–445), the availability of the previous assignment of the shorter peptide β(412–431) was helpful. A list of the assigned ^{1}H values for the peptides β(394–445), β(412–431), and α(404–451) is given in Tables ST1 and ST2 (see Supplementary material in Electronic Appendix). NMR analysis of these peptides without TFE proved difficult, similar to a β(400–445)-tubulin peptide (Reed et al., 1992), and was not further pursued.

Structure calculations

Calculations of peptide structures were carried out on a Silicon Graphics (Mountain View, California) Indigo computer using the program DIANA (Güntert et al., 1991). Distance constraints were derived from the 150 ms mixing time NOESY spectra. Observed NOEs were translated into upper limit distance constraints by visual inspection of their intensities using the following qualitative criterion: strong NOEs were set to distances lower than 0.30 nm; medium, lower than 0.35 nm, and weak lower than 0.40 nm. Pseudo-atom corrections were added to interproton distance restraints where necessary. Lower bounds between nonbonded atoms were set to the sum of van der Waals radii. ϕ angles were constrained to the range 0 to −180°, except for Gly and Asn residues.

Inhibition of microtubule polymerization by α- and β-tubulin C-terminal peptides

Microtubule protein (MTP) was prepared from bovine brain as described (Karr et al., 1982; de Pereda et al., 1995) in 100 mM Mes, 1 mM $MgCl_2$, 1 mM EGTA, 1 mM GTP, pH 6.7. Pellets of MTP were resuspended at 0 °C in 2 mL of 100 mM MES, 0.5 mM $MgCl_2$, 2 mM EGTA, 1 mM GTP, pH 6.4. The mixture was incubated on ice with gentle stirring for 20 min, centrifuged at 4 °C at 100,000 × g for 30 min and the supernatant adjusted to 2 mg/mL protein concentration, determined (Bradford, 1976) with purified tubulin as a standard. The samples, in a jacketed cuvette, were allowed to polymerize at 37 °C with and without peptide, monitoring the turbidity at different wavelengths in a Hewlett Packard 8452A spectrophotometer. The temperature was controlled with a circulating water bath and measured inside of the cuvette with a thermocouple.

Supplementary material in Electronic Appendix

^{1}H-NMR assignment of peptides (Tables ST1, ST2), HPLC characterization (Fig. SF1), and inhibition of microtubule assembly by the recombinant tubulin C-terminal peptides (Fig. SF2).

Acknowledgments

We are indebted to J.M. de Pereda, G. Pucciarelli, E. Nova, R. Martinez-Dalmau, M. Sjöberg, and J. Díaz, and all other members of the J.M.A. and O.M. labs, and D. Laurents for their help. This work was supported by grants from Agencia Española de Cooperacion Internacional, CSIC-Universidad de Chile, DGICyT PB95-0116, PB93-0189 and FONDECYT 1950556, 1981098.

References

Andreu D, de la Viña S, Andreu JM. 1988. Chemical synthesis of five tubulin antigenic sequences. *Int J Peptide Protein Res 31*:555–566.

Aranda C. 1994. Síntesis en *E. coli*, purificación y caracterización de un péptido carboxilo terminal de β-tubulina de pollo [Undergraduate Thesis]. Chile: Faculty of Pharmacy, University of Concepción.

Aue WP, Bartholdi E, Ernst RR. 1976. Two-dimensional spectroscopy. Application to nuclear magnetic resonance. *J Chem Phys 64*:2229–2246.

Bax A, Davis DG. 1985. Practical aspects of two-dimensional transverse NOE spectroscopy. *J Magn Reson 65*:355–360.

Berger B, Wilson DB, Wolf E, Tonchev T, Milla M, Kim PS. 1995. Predicting coiled coils by use of pairwise residue correlations. *Proc Natl Acad Sci USA 92*:8259–8263.

Bradford M. 1976. A rapid and sensitive method for the quantitation of microgram quantities of protein utilizing the principle of protein-dye binding. *Anal Biochem 72*:248–254.

Butner KA, Kirschner MW. 1991. Tau protein binds to microtubules through a flexible array of distributed weak sites. *J Cell Biol 115*:717–730.

Case DA, Dyson HJ, Wright PE. 1994. Use of chemical shifts and coupling constants in nuclear magnetic resonance structural studies on peptides and proteins. *Methods Enzymol 239*:392–416.

Chau MF, Radeke MJ, de Ines C, Barasoain I, Kohlstaedt L, Feinstein SC. 1998. The microtubule associated protein tau cross-links to two distinct sites on each α and β tubulin monomer via separate domains. *Biochemistry 37*:17692–17703.

Cowan NJ, Dobner PR, Fuchs S, Cleveland DW. 1983. Expression of human α-tubulin genes: Interspecies conservation of 3′-untranslated regions. *Mol Cell Biol 3*:1738–1745.

de la Viña S, Andreu D, Medrano FJ, Nieto JM, Andreu JM. 1988. Tubulin structure probed with antibodies to synthetic peptides. Mapping of three major types of limited proteolysis fragments. *Biochemistry 27*:5352–5365.

de Pereda JM, Andreu JM. 1996. Mapping surface residues of the tubulin dimer and taxol-induced microtubules with limited proteolysis. *Biochemistry 35*:14184–14202.

de Pereda JM, Billger M, Wallin M, Andreu JM. 1995. Comparative study of the colchicine binding site and the assembly of fish and mammalian microtubule proteins. *Cell Motil Cytoskeleton 30*:153–163.

de Pereda JM, Leynadier D, Evangelio J, Chacón P, Andreu JM. 1996. Tubulin secondary structure analysis, limited proteolysis sites and homology to FtsZ. *Biochemistry 35*:14203–14215.

Dyson HJ, Rance M, Houghten RA, Wright PE, Lerner RA. 1988. Folding of immunogenic peptide fragments of proteins in water solution. II. The nascent helix. *J Mol Biol 201*:201–217.

Eddé B, Rossier J, Le Caer JP, Promé JC, Desbruyères E, Gros F, Denoulet P. 1990. Posttranslational glutamylation of α-tubulin. *Science 247*:83–85.

Edelhoch H. 1967. Spectroscopic determination of tryptophan and tyrosine in proteins. *Biochemistry 6*:1948–1954.

Fleming LM, Johnson GVW. 1995. Modulation of the phosphorylation state of tau *in situ*: The roles of calcium and ciclyc AMP. *Biochem J 309*:41–47.

González C, Lagos, R, Monasterio O. 1996. Recovery of soluble protein after expression in *E. coli* depends on cellular disruption conditions. *Microbios 85*:205–212.

Güntert P, Braun W, Wüthrich KJ. 1991. Efficient computation of three-dimensional protein structures in solution from NMR data using the program DIANA and the supporting programs CALIBA, HABAS and GLOMSA. *J Mol Biol 217*:517–530.

Gustke N, Trinczek J, Biernat J, Mandelkow EM, Mandelkow E. 1994. Domains of τ protein interactions with microtubules. *Biochemistry 33*:9511–9522.

Jiménez MA, Bruix M, González C, Blanco FJ, Nieto JL, Herranz J, Rico M. 1993. CD and 1H-NMR studies on the conformational properties of peptide fragments from the C-terminal domain of thermolysin. *Eur J Biochem 211*:569–581.

Jiménez MA, Muñoz V, Rico M, Serrano L. 1994. Helix stop and start signals in peptides and proteins. The capping box does not necessarily prevent helix elongation. *J Mol Biol 242*:487–496.

Johnson ML, Correia JJ, Yphantis DA, Halvorson HR. 1981. Analysis of data from analytical ultracentrifugation by non-linear least squares techniques. *Biophys J 36*:575–588.

Karr TL, White HD, Coghlin BA, Purich DL. 1982. A brain microtubule protein preparation depleted of mitochondrial and synaptosomal components. *Methods Cell Biol 24*:51–60.

Kotani S, Kawai G, Yokoyama S, Murofushi H. 1990. Interaction mechanism between microtubule-associated proteins and microtubules. A proton nuclear resonance analysis on the binding of synthetic peptide to tubulin. *Biochemistry 29*:10049–10054.

Krueger AK, Bhatt H, Landt M, Easom RA. 1997. Calcium-stimulated phosphorylation of MAP-2 in pancreatic bTC3-cells is mediated by Ca^{2+}/calmodulin-dependent kinase II. *J Biol Chem 272*:27464–27469.

Kumar A, Ernst RR, Wüthrich K. 1980. A two-dimensional nuclear Overhauser enhancement (2D NOE) experiment for the elucidation of complete proton-proton cross-relaxation networks in biological macromolecules. *Biochem Biophys Res Commun 95*:1–6.

Larcher JC, Boucher D, Lazereg S, Gros F, Denoulet P. 1996. Interaction of kinesin motor domains with α- and β-tubulin subunits at a Tau-independent binding site. *J Biol Chem 271*:22117–22124.

Laue TM, Shah DB, Ridgeway TM, Pelletier SL, Horton JC. 1992. Computer-aided interpretation of analytical sedimentation data for proteins. In: Harding SE, Rowe AJ, eds. *Analytical ultracentrifugation in biochemistry and polymer science*. United Kingdom: Royal Society of Chemistry. pp 90–125.

Littauer UZ, Giveon D, Thierauf M, Ginzburg I, Ponstingl H. 1986. Common and distinct tubulin binding sites for microtubule-associated proteins. *Proc Natl Acad Sci USA 83*:7162–7199.

Lobert S, Hennington BS, Correia JJ. 1993. Multiple sites of subtilisin cleavage of tubulin: Effects of divalent cations. *Cell Motil Cytoskeleton 25*:282–297.

Ludueña RF. 1998. Multiple forms of tubulin: Different gene products and covalent modifications. *Intl Rev Cytol 178*:207–275.

Luo P, Baldwin RL. 1997. Mechanism of helix induction by trifluoroethanol: A framework for extrapolating the helix-forming properties of peptides from trifluorethanol/water mixtures back to water. *Biochemistry 36*:8413–8421.

Lupas A, Van Dyke M, Stock J. 1991. Predicting coiled coils from protein sequences. *Science 252*:1162–1164.

Mandelkow E, Johnson J. 1998. The structural and mecanochemical cycle of kinesin. *Trends Biochem Sci 23*:429–433.

Marion D, Wüthrich K. 1983. Application of phase-sensitive two-dimensional correlated spectroscopy (COSY) for measurements of proton–proton spin–spin coupling constants. *Biochem Biophys Res Commun 113*:967–974.

Marya PK, Syed Z, Fraylich PE, Eagles PA. 1994. Kinesin and tau bind to distinct sites on microtubules. *J Cell Sci 107*:339–344.

Mejillano MR, Himes RH. 1991. Assembly properties of tubulin after carboxyl group modification. *J Biol Chem 266*:657–664.

Merutka G, Dyson HJ, Wright PE. 1995. "Random coil" 1H chemical shifts obtained as a function of temperature and trifluoroethanol concentration for the peptide series GGXGG. *J Biomol NMR 5*:14–24.

Minton AP. 1994. Conservation of signal: A new algorithm for the elimination of the reference concentration as an independently variable parameter in the analysis of sedimentation equilibrium. In: Schuster TM, Laue TM, eds. *Modern analytical ultracentrifugation*. Boston: Birkhäuser. pp 81–93.

Muñoz V, Serrano L. 1994. Elucidating the folding problem of helical peptides using empirical parameters. *Nat Struct Biol 1*:399–409.

Nelson JW, Kallenbach NR. 1986. Stabilization of ribonuclease S-peptide α-helix by trifluoroethanol. *Proteins 1*:211–217.

Nogales E, Wolf SG, Downing KH. 1998. Structure of the $\alpha\beta$-tubulin dimer by electron crystallography. *Nature 391*:199–203.

Novella IS, Andreu JM, Andreu D. 1992. Chemically synthesized segment 182–235 of tau protein and analogue peptides are efficient microtubule assembly inducers of low apparent specificity. *FEBS Lett 311*:235–240.

O'Brien T, Salmon ED, Erickson HP. 1997. How calcium causes microtubule depolymerization. *Cell Motil Cytoskeleton 36*:125–135.

Ortiz M, Lagos R, Monasterio O. 1993. Interaction between the C-terminal peptides of tubulin and tubulin-S detected with the fluorescent probe 4′,6-diamidino-2-phenylindole. *Arch Biochem Biophys 303*:159–164.

Paschal BM, Obar RA, Vallee RB. 1989. Interaction of brain cytoplasmic dynein and MAP2 with a common sequence at the C-terminus of tubulin. *Nature 342*:569–572.

Perczel A, Park K, Fasman GD. 1992. Analysis of the circular dichroism spectra of proteins using the convex constraint algorithm: A practical guide. *Anal Biochem 203*:83–93.

Ponstingl H, Little M, Khrauhs E, Kempf T. 1979. Carboxy-terminal amino acid sequence of α-tubulin from porcine brain. *Nature 282*:423–424.

Redecker V, Melki R, Promé D, Le Caer JP, Rossier J. 1992. Structure of tubulin C-terminal domain obtained by subtilisin treatment. The major α and β tubulin isotypes from pig brain are glutamylated. *FEBS Lett 313*:185–192.

Reed J, Hull WE, Ponstingl H, Himes RH. 1992. Conformational properties of the β(400–436) and β(400–445) C-terminal peptides of porcine brain tubulin. *Biochemistry 31*:11888–11895.

Rost B, Sander C. 1993. Prediction of protein secondary structure at better than 70% accuracy. *J Mol Biol 232*:584–599.

Sackett DL, Bhattacharyya B, Wolff J. 1985. Tubulin subunit carboxyl termini determine polymerization efficiency. *J Biol Chem 260*:43–45.

Serrano L, de la Torre J, Maccioni RB, Avila J. 1984. Controlled proteolysis of tubulin by subtilisin: Localization of the site for MAP2 interaction. *Biochemistry 23*:4675–4681.

Serrano L, Valencia A, Caballero R, Avila J. 1986. Localization of the high affinity calcium-binding site on tubulin molecule. *J Biol Chem 261*:7076–7081.

Solomon F. 1977. Binding sites for calcium on tubulin. *Biochemistry 16*:358–363.

Soto C, Rodriguez PH, Monasterio O. 1996. Calcium and gadolinium ions stimulate the GTPase activity of purified chicken brain tubulin through a conformational change. *Biochemistry 35*:6337–6344.

Studier FW, Moffatt BA. 1986. Use of bacteriophage T7 RNA polymerase to direct selective high-level expression of cloned genes. *J Mol Biol 189*:113–130.

Tabor S, Richardson CC. 1985. A bacteriophage T7 RNA polymerase/promoter system for controlled exclusive expression of specific genes. *Proc Natl Acad Sci USA 82*:1074–1078.

Valenzuela P, Quiroga M, Zaldivar J, Rutter WJ, Kirschner MW, Cleveland DW. 1981. Nucleotide and corresponding amino acid sequences encoded by α- and β-tubulin mRNAs. *Nature 289*:650–655.

Wishart DS, Sykes BD. 1994. Chemical shifts as a tool for structure determination. *Methods Enzymol 239*:363–392.

Wüthrich K. 1986. *NMR of proteins and nucleic acids*. New York: J. Wiley and Sons.

Wüthrich K, Billeter M, Braun W. 1984. Polypeptide secondary structure determination by nuclear magnetic resonance observation of short proton–proton distances. *J Mol Biol 180*:715–740.

Yang JT, Chuen-Shang CW, Martinez HM. 1986. Calculation of protein conformation from circular dichroism. *Methods Enzymol 130*:208–269.